
smICA: an open source repository for mapping the concentration of fluorescently labeled molecules in living cells on the basis of confocal imaging combined with time-correlated single-photon counting

Tomasz Kalwarczyk^{1,*}, Grzegorz Bubak¹, Jarosław Michalski¹, Karina Kwapiszewska¹, Marta Pilz¹, Adam Mamot², Jacek Jemielity², Robert Hołyst¹,

**1 Institute of Physical Chemistry, Polish Academy of Sciences
Kasprzaka 44/52 01-224, Warsaw, Poland.**

**2 Centre of New Technologies, University of Warsaw, Banacha 2c Street,
02-097 Warsaw**

* tkalwarczyk@ichf.edu.pl

Abstract

Advanced microscopy techniques are essential for visualizing and tracking cellular components and molecules in biomedical research. However, conventional fluorescence microscopy methods often struggle with accurately measuring molecule concentrations in cells. To overcome these limitations, we introduce a novel approach that integrates laser scanning confocal microscopy with time-correlated single photon counting (TCSPC), supported by an open-source analysis tool called smICA (single-molecule Image to Concentration Analyzer). Our method, validated against traditional fluorescence correlation spectroscopy (FCS), offers enhanced accuracy in determining fluorescent molecule concentrations, particularly in cases where molecules are immobile or unevenly distributed. This is demonstrated using fluorescently labeled mRNA in living cells, highlighting the approach's effectiveness.

Introduction

Advanced microscopes are necessary for quantitative biological studies, especially when visualizing cells, localizing and tracking single molecules, or analyzing their concentration. Fluorescence microscopy, particularly confocal microscopy, has become a standard tool in biomedical research. Numerous techniques have evolved from traditional laser scanning confocal microscopy (LSCM), including fluorescence correlation spectroscopy (FCS),^{3,4,10,11} raster image correlation spectroscopy (RICS),¹ and fluorescence lifetime imaging microscopy (FLIM). These techniques are based on time-correlated single photon counting (TCSPC), which enables the tracking of photons emitted by fluorescence molecules, one by one, in time.

There are various ways to monitor the concentration of fluorescent molecules. Qualitatively, fluorophore's concentration in the given region of the sample can be deduced from the fluorescence intensity as it is proportional to concentration. However, obtaining quantitative measurements is more challenging, and FCS is the more appropriate technique of choice. The disadvantage of the correlation-based methods is that they are limited to mobile molecules and are blind to molecules that are, for some reason, immobile. Moreover, the traditional FCS measurements only

offer information from a single spot. Although, there were attempts to perform multipoint FCS,^{6,14,18} the technique requires customized equipment and is difficult to attempt on the commercially available setups. Therefore, the representative FCS measurements can only be conducted under the assumption of homogenous analyte distribution within the sample. The limitations, including the restriction to mobile species, spatial constraints, and compartmentalization make quantifying concentrations in living cells particularly challenging. This difficulty arises because target biomolecules often localize within specific subcellular structures and organelles, resulting in an uneven distribution throughout the cell. Analyzing a map or the probe's concentration distribution is more desirable in such cases.

An example of a qualitative approach to studying the number of fluorescent molecules registered on a given image was proposed by Vukojevic et al.¹⁶ The authors used Poissonian statistics to measure the average number of molecules in the observation volume without temporal or spatial correlation of the images. Due to strong deviations from the Poissonian statistics lying on its ground, the method is limited to two orders of magnitude of the analyte concentration (1-100 nM). The method described by Vukojevic et al.¹⁶ has the same grounds as the Number and Brightness (N&B) method proposed by the group of Gratton² using the relation between the mean and variance of the fluorescence signal to the molecular brightness and number of fluorescent molecules. The advantage of the N&B is that the molecular brightness of the molecule of interest does not need to be known a priori as it is determined from the fluorescence fluctuation signal. Moreover, the method discriminates between the mobile and immobile molecule fractions. Both methods, however, do not consider factors such as the autofluorescence of biological samples or the cross-talk between fluorescent dyes when measurements are performed in the multi-color mode.

We propose an alternative approach for determination of the concentration of fluorophores instead of their number. We combine the laser scanning confocal microscope with the time-correlated single photons counting (TCSPC) acquisition method. We assume that the molecular brightness of the analyte is known a priori and is spatially and temporarily constant. We provide an open-source smICA (single-molecule Image to Concentration Analyser) repository consisting of sets of graphical user interfaces (GUIs)⁷ and perform validation test comparing the concentration determined with the proposed methodology with the well known FCS method. Finally we provide the proof of concept results for the method by applying it to study the concentration of fluorescently labeled mRNA in living cells. We observed that many fluorescently labeled mRNA molecules are entrapped in subcellular structures or organelles, making them immobile and significantly non-uniformly distributed. While we do not discuss the biological aspects of this phenomenon, it helps us to show that our imaging method outdoes the FCS measurements, which may lead to significant underestimation of the mean mRNA concentration.

Materials and methods

Cell culture

Human lung carcinoma cells (A549 line) were obtained from the American Type Culture Collection (ATCC). The cells were cultured in DMEM (Institute of Immunology and Experimental Technology, Wrocław, Poland) supplemented with 10% fetal bovine serum, L-glutamine (2 mM), penicillin (100 $\mu\text{g}/\text{ml}$), and streptomycin (100 $\mu\text{g}/\text{ml}$) from Sigma-Aldrich. The culture was maintained at 37°C in a 5% CO_2 humidified atmosphere. Passaging was carried out at approximately 80% confluence

every 2-3 days using 0.25% Trypsin-EDTA solution (Sigma-Aldrich) and PBS (Sigma-Aldrich).

mRNA injections

The A549 cells for microinjections were plated 1 or 2 days before the measurements on a 35 mm glass bottom cell culture dish (glass coverslip bottom, 0.17 μm , ibidi, Germany) to grow to approximately 50-70 % confluence. Microinjections were performed by the Femtojet system (Eppendorf) using disposable sterile injection glass capillaries (Femtotip II, Eppendorf, 0.5 μm inner and 0.7 μm outer diameter). The injection time was set to 0.1 s. Before FCS measurements but after microinjections, the growth medium in the culture dish was washed out and replaced with PBS buffer containing Ca^{2+} and Mg^{2+} ions (Sigma-Aldrich).

Experimental setups

The measurements were performed using the NIKON C1 and NIKON A1 confocal microscopes. Both setups are additionally equipped with the TCSPC acquisition unit (LSM Upgrade-kit from PicoQuant, Germany). The LSM units are composed of three pulsed diode lasers (485, 561, and 641 nm of wavelength) controlled by the PDL 828 "SEPIA II" controller, the TCSPC module PicoHarp 300, and the pair of single photon avalanche diode - SPAD, detectors with appropriate filters. We used the PLAN APO water immersion objective x60 NA 1.20 in all experiments. Both confocal systems are equipped with an incubator, allowing for temperature control. Measurements in buffers were performed at 298 K, while experiments were conducted at 309 K.

Materials

The fluorescently labeled mRNA (Cy5-m7GRNAegfp, stained with sulfo-Cy5 at the 5' Cap) was synthesized and purified according to the previously published procedure¹². Briefly, mRNA was in vitro transcribed in the presence of azido-modified cap analog (N3-m7GpppG) and subsequently isolated with spin columns. After labeling with sulfo-Cy5-DBCO, the product was isolated with HPLC and characterized with gel electrophoresis. The TRITC labeled dextran of molecular weights 4.4 kDa, 40 kDa and 155 kDa were bought from Sigma-Aldrich.

Fluorescence correlation spectroscopy - calibration, brightness and concentration

Before each experiment, calibration measurements were performed using the fluorescence correlation spectroscopy technique (FCS). Depending on the laser and the fluorophore under study, we performed calibration using Rhodamine 110 (for 485 nm laser line), Rhodamine B (561 nm laser line) and Alexa Fluor 647 (for 641 nm laser line). The diffusion coefficients for both dyes at 25 degrees were taken from the reference 8. For measurements in living cells, the calibration measurements were performed at 36 degrees, and the diffusion coefficients were recalculated, including the change in temperature and viscosity. We get the structure parameter κ (fixed in target FCS measurements), the width of the focal volume, ω , and focal volume, V_{eff} from the calibration measurements. Then we performed FCS measurements of our samples to determine the molecular brightness, B of used probes. We obtained the average number of molecules in the confocal focus, N_m from analysing FCS auto-correlation curve and photon-counts per second, Cnt_{rate} from the raw FCS time-trace signal. To determine the Cnt_{rate} for a given FCS measurement, we calculated the cumulative

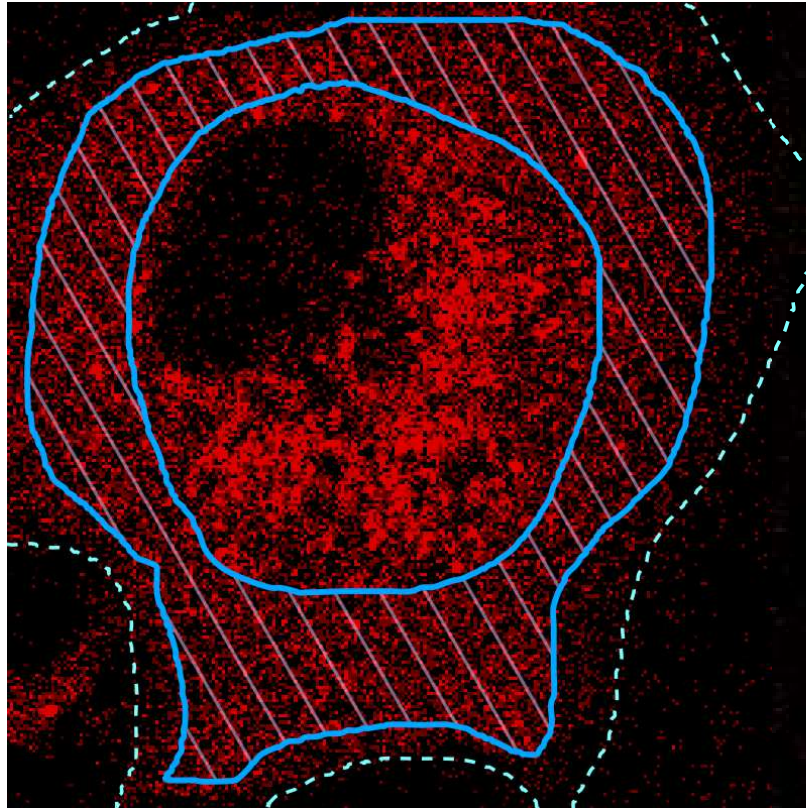


Figure 1. The striped region marked in the figure relates to the places where the FCS measurements were typically performed. The dashed curve represents the cell boundary. The FCS measurements were chosen to omit the endoplasmic reticulum and nucleus.

sum of detected photons for each second of measurement and fitted the result with homogeneous linear function ($y = ax$). Cnt_{rate} is equal to the slope of the fitted function. The brightness is given as $B = Cnt_{rate}/N_m$. For each sample we performed a series of FCS measurements and calculated an average value of B from the series.

FCS measurements in cells were performed in the cell cytoplasm trying to avoid the endoplasmic reticulum and the bright spots where the accumulation of mRNA molecules is expected. The striped region of the cell marked in Figure 1 depicts region of the cell where typical FCS measurements were conducted.

Concentration imaging methodology

The single-photon fluorescence imaging data, if not properly analyzed, consists of artifacts originating from the photophysics (triplet states or photobleaching), samples (dye crosstalk, autofluorescence), and detectors (afterpulsing). Quantitative analysis of dye concentration requires recognition of each artifact source and reduction of their influence on the experimental data. Below, we describe our strategy to tackle the challenge.

The scheme of the methodology is depicted in Figure 2. First, we use standard FCS measurements to calibrate the confocal volume and determine the molecular brightness, B , of the fluorophore used in further experiments. The molecular brightness depends on the power of the incident light and the experimental setup settings. Therefore, measuring under the same conditions as the final experiments is recommended. We further assume that in the sample, B does not change, neither

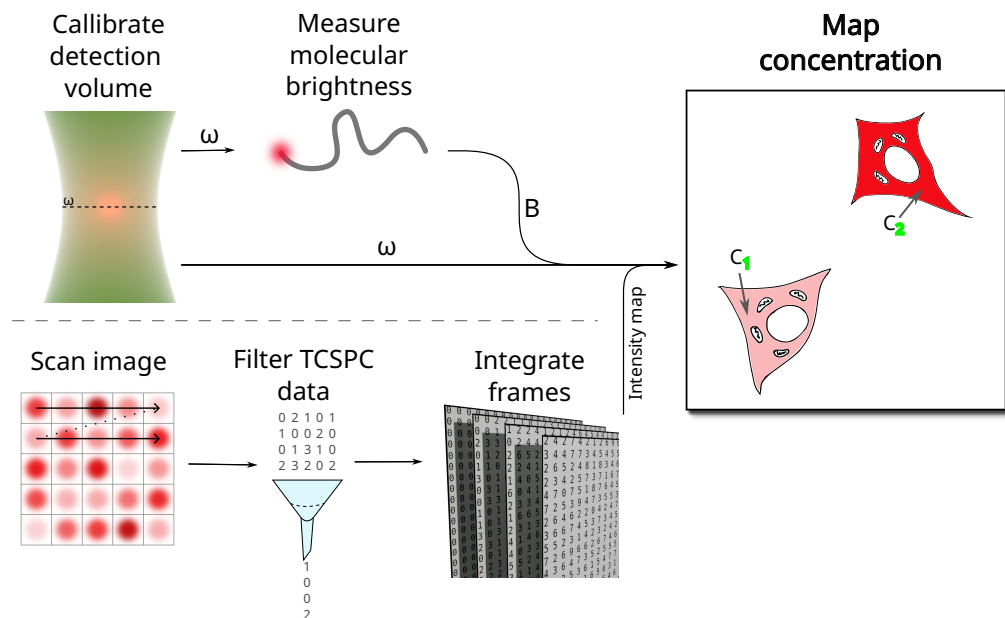


Figure 2. The figure shows the workflow scheme used in the concentration imaging method. First, we calibrate the FCS setup using a dye with a known diffusion coefficient. From calibration measurements, we get ω - the width of the focal volume. Next, we performed the FCS measurements on the target samples to find the molecular brightness, B . Finally, the raster imaging was performed using the laser scanning confocal microscopy equipped with the spad detectors. The raw data acquired during the scanning was further filtered from unwanted background, afterpulsing, or autofluorescence photons. The filtered signal was combined into frames and integrated over all frames. Knowing the ω and brightness, we calculated the mean concentration of fluorophores in each pixel averaged over the data acquisition time.

spatially nor temporally.

After calibration, we perform the LSCM imaging combined with the SPAD detectors utilizing the TCSPC method. Standard LSCM hardware provides filtration via optical filters and dichroic mirrors. The TCSPC method used in the time-tagged time-resolved (TTTR) mode,¹⁷ additionally, allows filtering fluorescence data by methods relying on the fluorescence decay pattern such as fluorescence lifetime filtering (commonly used in fluorescence lifetime correlation spectroscopy)^{5,9} or the pulsed interleaved excitation combined with the time gating.

The raw TTTR data are extracted from the binary *.ptu* files, optionally filtered, integrated over all registered frames, and combined into the image. Each image pixel contains a total number of photons registered at a given spot in the sample. Next, for each pixel, we calculate the effective number of detected molecules, N_m , using the fluorophore's molecular brightness, B . The mean number of molecule detected at a given spot is given as $N_m = N_p / (B \Delta t N_f)$, where Δt stands for the pixel dwell time and N_f is the number of frames acquired. Finally, knowing the dimensions of the effective focal volume, we calculate the mean concentration per pixel; $C_{im} = N_m / (N_A V_{eff})$, where N_A is the Avogadro number and V_{eff} corresponds to the volume of the focal spot obtained from the of FCS calibration measurements.

The graphical user interface

The tool for concentration imaging consists of three scripts. Although the scripts perform simple tasks, they are designed to be as intuitive as possible. We aim to use them by users who are not trained in programming and allow them to analyze large amounts of data files in a repeatable manner. Here, we briefly describe the scripts, while detailed step-by-step manuals are available at the repository site.⁷ All scripts are based on the Dear PyGUI - the graphical user interface toolkit(GUI) for Python, making them fast, dynamic, and intuitive.

The first GUI script, `EXTRACT_AND_FILTER_PTU`, is dedicated to extracting the raw TTTR data from the binary `.ptu` file where the data acquired by the commercial, FLIM/FCS dedicated SymPhoTime software are stored. The data are extracted with the help of the `readPTU_FLIM` library¹⁵ designed to read the `.ptu` files. Read TTTR data gathered in different channels are split. In each channel, the user can filter the data using the time gating method or by applying the statistical filters according to the algorithm described in references 5 and 9. As an output, the script returns a series of files consisting of the following: (i) an array the number of photons registered in each pixel of the unfiltered image (one file per channel), (ii) an array for intensity values (number of photons after filtration) per pixel (one file per channel), (iii) an array for fluorescence average lifetime values per pixel after filtration (one file per channel), (iv) the decay pattern for each channel (separate files), (v) a `.png` file that can be further used to set the region of interest - ROI. The second GUI script is called `REWRITE_ROI`. The use of this script is optional and is related to the ROI. The ROI used in the further analysis can be selected directly in the SymPhoTime at the data acquisition stage. However, when a lot of data is acquired and time between subsequent data points is crucial, selecting the ROI after the data acquisition is more desired. In our experiments, we used the ImageJ software to read the `.png` files generated by the `EXTRACT_AND_FILTER_PTU` script and then create the ROI as a mask, which was further saved as the text image. If the ROI data are not created using the SymPhoTime software, using the `REWRITE_ROI` script is necessary. Our script transcribes the ImageJ-generated files into the SymPhoTime format.

The third script performs all calculations required to translate the number of photons into the concentration. The user can select the set of roi files (by choosing the folder) corresponding to the analyzed ptu files. The FCS calibration parameters, including the focal volume structure parameter, κ , the lateral size of the focal volume, ω , and the molecular brightness, B , can be manually added or loaded from the `.json` file. The calculations are performed for all files selected by the user. As an output, the script returns the text files containing (i) an array of the number of molecules per pixel, (ii) an array of the mean concentration of molecules per pixel, (iii) the table in the user-desired format (`.csv`, `.xlsx`, `.dat`, `.pickle`¹). The output table consisting of the File name, channel number, the mean number of counts (photons), mean number of molecules per pixel, mean concentration per pixel, and the corresponding standard deviations. All mean values correspond to the average over the entire image or ROI (if selected).

Results and discussion

Validation and tests

To validate the determination of the concentration, we designed experiments where we changed the fluorophore's concentration, power of the laser P (measured at the

¹This is the binary file storing the pandas DataFrame.

sample), the pixel dwell time - Δt , and the size of the pixel Δx or, more precisely, the scan velocity defined as $\Delta x/\Delta t$.²

We measured a well-defined probe - the dextran polymer of molecular weight of 155 kg/mol labeled with the TRITC dye. This polymer is characterized by the hydrodynamic radius of the order of 9 nm. The measurements on dextrans were performed in water at 25°C. The concentration of the polymers varied from ~6 to ~100 nM. The laser power, P , was changed between 5 to 40 μW , which corresponded to the peak focal irradiance I_0 ,³ varying from 0.07 to 0.5 $\text{mW}/\mu\text{m}^2$. The pixel dwell time was changed between 3.12 μs to 60 μs , and the scan velocity changed between 0.4 $\text{nm}/\mu\text{s}$ to 64.1 $\text{nm}/\mu\text{s}$. At low polymer concentrations, laser power, and short Δt , the signal-to-noise ratio, SNR, was close to unity and the probability of detection of a photon from the fluorescent molecule was below unity. For example, the average number of photons, $N_p=0.013$, expected to be observed per one dextran molecule at $P=5 \mu\text{W}$ ($B=4260$ photons/molecule/s) and $\Delta t = 3.12 \mu\text{s}$. For the highest laser power of $P=40 \mu\text{W}$ ($B=12300$ photons/molecule/s) and $\Delta t = 60 \mu\text{s}$, $N_p=0.74$. To increase the chance of detecting any photon, we integrated the signal over ten frames in post-acquisition processing, increasing the expected N_p values by ten times.

Post-acquisition processing also includes the filtration of unwanted photons originating from afterpulsing, the sample's autofluorescence, or the dye-dye crosstalk. Technically, the filtration procedure is performed on the raw TCSPC signal before the over-all-frames integration. In the EXTRACT_AND_FILTER_PTU, GUI, we implemented two methods of photons filtering, both of which relied on TCSPC data. The first method is based on the fluorescence lifetime decay pattern^{5,9}, where the properly calculated weights are applied to each registered photon. The filtering was applied to the FITC-labeled dextran data and compared to the non-filtered data; see Figure 3a. We calculated the concentration of fluorescent dextran molecules for each image pixel and then averaged over all pixels. We further compared the mean value to the concentration obtained from imaging, C_{im} with the one determined using FCS, C_{FCS} on the same sample at the same concentration and laser power conditions, by calculating their ratio, $C_{\text{im}}/C_{\text{FCS}}$. We found that independently on the experimental conditions (laser's power, pixel dwell time, pixel size or concentration) the $C_{\text{im}}/C_{\text{FCS}}$ oscillates around unity. The distribution of the $C_{\text{im}}/C_{\text{FCS}}$ values for all measurements are depicted as violin plots in Figure 3b. During image analysis, we also checked the influence of the number of pixels used in analysis (size of the region of interest - ROI). We found that the filtration procedure caused over-filtration of the fluorescence signal, manifested as systematically lowered values of the $C_{\text{im}}/C_{\text{FCS}}$ ratio. Interestingly the size of the ROI do not influence the results significantly. We used several sizes of square regions of interest differing in the number of pixels, N_{px} , varying from 16^2 to 256^2 pixels ($N_{\text{px}}=256^2$ refers to the full frame). In both filtered and non-filtered data, the ROI size did not influence the mean value of the $C_{\text{im}}/C_{\text{FCS}}$ ratio, but data variance decreases with the ROI's dimension. For the ROI size $\sqrt{N_{\text{px}}} \geq 48$, the differences in data distribution were unrecognizable; cf. Figure 3b. The mean value of the $C_{\text{im}}/C_{\text{FCS}}$ ratio for all non-filtered data is close to 1.05, with the square root of the variance (σ) at the level of 0.23 for the smallest ROI and not higher than 0.19 for $\sqrt{N_{\text{px}}} \geq 48$. On the contrary, the filtered data for all ROI sizes exhibits σ values not higher than 0.17, but the mean value of the $C_{\text{im}}/C_{\text{FCS}}$ ratio did not exceed 0.78.

The second type of filter implemented in the EXTRACT_AND_FILTER_PTU GUI is based on the time-gating method, which is dedicated to cases when the crosstalk between fluorophores occurs. To verify the photon filtering efficiency under

²The variable controlled experimentally in the hardware setup is Δx . We assume, however, that the effective size of the pixel is equal to the focal volume illuminated within the time Δt . The focal volume is determined from the FCS calibration measurements.

³ $I_0 = 2P/(\pi\omega_0^2)$, where ω_0 stands for the radius of the focal volume.

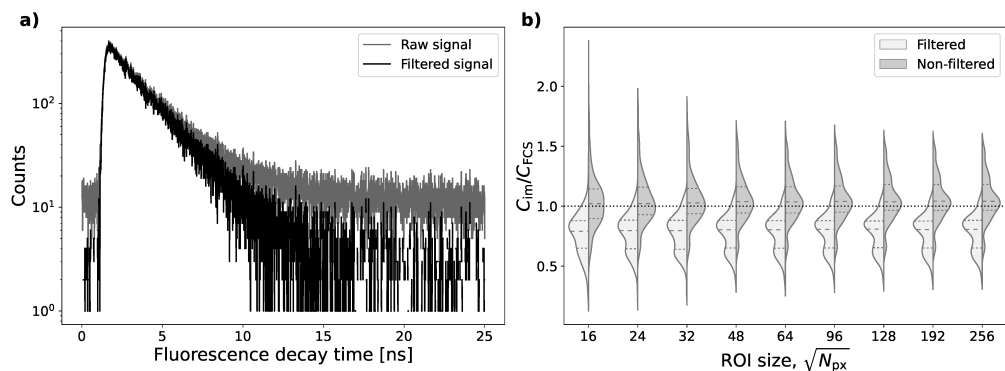


Figure 3. Figure **a** depicts a plot of the fluorescence decay patterns for the raw signal and the filtered signal acquired for the TRITC-labeled dextran polymer. We applied the filtering based on the afterpulsing and background removal according to the algorithm described in references 5, and 9. Panel **b** shows violin plots representing the distributions of the C_{im}/C_{FCS} ratio obtained for different region-of-interest sizes. ROI size $\sqrt{N_{px}} = 256$ corresponds to the full frame.

the dye-dye crosstalk conditions, we performed test measurements on the cells where two types of fluorophores were present, the EGFP and the TRITC-labeled dextran. The EGFP was synthesized in cells after injection of the mRNA encoding the EGFP sequence. The TRITC-labeled dextran was mixed with the non-labeled mRNA at known proportions and injected into cells. Mixing of the mRNA and dextran allowed us to estimate the concentration of the injected mRNA. To separate the excitation events between the laser lines, we operated in the pulse interleaved excitation, PIE, mode, allowing us to shift the consecutive laser's pulses in time. We used the shift between the equal to 25 ns, and the delay time between pulses of the same laser of 50 ns. We analyzed the data from sixteen different cells. The power of the lasers was set to 10 μ W for the green laser ($\lambda = 561$ nm) and 2 μ W for the blue laser ($\lambda = 485$ nm). The images were acquired for $\Delta x = 399$ nm, $\Delta t = 8$ μ s and integrated over 100 frames.

Figures 4**a** and **b** show exemplary fluorescence decay patterns of the TRITC-labeled dextran and the EGFP, acquired with two SPAD detectors corresponding to the TRITC and EGFP channels. The pulse of the green laser is shifted by +25 ns with respect to the pulse of the blue laser. To filter out the photons originating from the dye-dye crosstalk recorded in the TRITC channel, we selected the decay-time range from 25-50 ns; Figure 4**a**. Consequently, the range of decay times for the EGFP channel was chosen as between 0 and 25 ns; 4**b**. Figure 4**c** compares the C_{im}/C_{FCS} for the filtered and non-filtered signals for FITC-labeled dextran and eGFP, respectively. Although the differences in the C_{im}/C_{FCS} ratio for the filtered and non-filtered are not very pronounced, the drop in the values agrees with the differences in intensities from the crosstalking fluorophores.

Example of implementation

We apply the described methodology to the quantitative measurements of the concentration of the fluorescently labeled mRNA and its changes upon the time after injection. The cells were injected with CAP-modified mRNA fluorescently labeled with the sulfo-Cy5 dye.¹² The mRNA was encoding the green fluorescent protein. The initial concentration of injected mRNA was around 100 nM and varied from cell to cell. Concentration imaging was performed on three cells. Between the image acquisition, we performed FCS measurements to determine the concentration of mRNA molecules

freely diffusing along the cytoplasm. Figure 5 (bottom panel) compares the data gathered using FCS and concentration imaging. The FCS data are significantly underestimated due to the accumulation of the mRNA molecules inside granules. The top panel of Figure 5 shows concentration maps acquired at the beginning, in the middle, and at the end of data acquisition; the exact time after mRNA injection is marked in the top right corner of the histogram of concentration determined for each pixel. We exclude the photobleaching of the dye to be responsible for the decay of the concentration observed. Instead, we attribute this change to the degradation of the mRNA molecules, after which the free dye is immediately removed from the cell. To exclude the photobleaching as a main source of the concentration decay, we analyzed the change in the total number of photons registered in the first and last frame of the data point.¹³ Although there is a systematic decay in the number of photons between the first and last frame, the change between the data points (during which the sample was not illuminated), its value is too small in comparison to the change between consecutive data points, to be considered as the main cause of the observed decay. Figure 6 shows data representing the total amount of photons during the acquisition of each data point's first and last frames.

Conclusions

We presented a methodology and the GUI scripts for mapping the fluorophore's concentration in living cells. The methodology requires the calibration of the confocal volume utilizing standard FCS measurement and assumes that the brightness of the fluorophore is constant. Meeting both requirements allows us to determine the mean concentration per pixel, averaged over the data acquisition time. Therefore, an output contains information about the average concentration over the entire cell/ROI and the concentration map across the cell/ROI. As a proof of concept, we applied the method to monitor the changes in the concentration of fluorescently labeled mRNA in living cells. Observed changes in mRNA suggest that the presented methodology is a promising tool for quantitative single-cell studies. Finally, narrowing ROI to specific organelles can provide insight into more detailed topics, including but not limited to protein expression, degradation of biomolecules, monitoring of enzymatic reactions, and investigation of probes' affinity of probes for specific cellular targets.

Acknowledgments

Research funded by the Polish Science Fund within the framework of the Virtual Research Institute; grant WIB-1/2020-O11 - WIB_HERO.

Authors contribution

TK: Methodology, Software, Validation, Formal analysis, Investigation, Data Curation, Visualization, Supervision, Writing - Original Draft, Writing - Review & Editing. **GB:** Investigation, Data Curation, Methodology, Validation, Writing - Original Draft, Writing - Review & Editing. **JM:** Investigation, Visualization, Data Curation, Writing - Review & Editing. **KK:** Investigation, Data Curation, Methodology, Software (testing), Writing - Original Draft, Writing - Review & Editing. **MP:** Methodology, Software (testing), Writing - Review & Editing. **AM:** Resources. **JJ:** Resources, Funding acquisition. **RH:** Funding acquisition, Writing - Review & Editing.

References

1. CM Brown, RB Dalal, B Hebert, MA Digman, AR Horwitz, and E Gratton. Raster image correlation spectroscopy (rics) for measuring fast protein dynamics and concentrations with a commercial laser scanning confocal microscope. *Journal of microscopy*, 229(1):78–91, 2008.
2. Michelle A Digman, Rooshin Dalal, Alan F Horwitz, and Enrico Gratton. Mapping the number of molecules and brightness in the laser scanning microscope. *Biophysical journal*, 94(6):2320–2332, 2008.
3. Måns Ehrenberg and Rudolph Rigler. Rotational brownian motion and fluorescence intensify fluctuations. *Chemical Physics*, 4(3):390–401, 1974.
4. Elliot L Elson and Douglas Magde. Fluorescence correlation spectroscopy. i. conceptual basis and theory. *Biopolymers: Original Research on Biomolecules*, 13(1):1–27, 1974.
5. Jörg Enderlein and Ingo Gregor. Using fluorescence lifetime for discriminating detector afterpulsing in fluorescence-correlation spectroscopy. *Review of scientific instruments*, 76(3), 2005.
6. Rémi Galland, Jie Gao, Meike Kloster, Gaetan Herbomel, Olivier Destaing, Martial Balland, Catherine Souchier, Yves Usson, Jacques Derouard, Irène Wang, et al. Multi-confocal fluorescence correlation spectroscopy: experimental demonstration and potential applications for living cell measurements. *arXiv preprint arXiv:1112.5392*, 2011.
7. GUI. The source code is available at <https://github.com/TKmist/smICA>. The bundle consists of three scripts: EXTRACT_AND_FILTER_PTU, REWRITE_ROI, and Phot2Conc. See <https://github.com/TKmist/smICA/blob/main/README.md> for more details.
8. Peter Kapusta. Absolute diffusion coefficients: Compilation of reference data for fcs calibration. *Application Note. PicoQuant GmbH, Germany*, pages 1–2, 2010.
9. Peter Kapusta, Michael Wahl, Aleš Benda, Martin Hof, and Jörg Enderlein. Fluorescence lifetime correlation spectroscopy. *Journal of fluorescence*, 17:43–48, 2007.
10. Dennis E Koppel. Statistical accuracy in fluorescence correlation spectroscopy. *Physical Review A*, 10(6):1938, 1974.
11. Douglas Magde, Elliot Elson, and Watt W Webb. Thermodynamic fluctuations in a reacting system—measurement by fluorescence correlation spectroscopy. *Physical review letters*, 29(11):705, 1972.
12. Adam Mamot, Pawel J Sikorski, Aleksandra Siekierska, Peter de Witte, Joanna Kowalska, and Jacek Jemielity. Ethylenediamine derivatives efficiently react with oxidized rna 3' ends providing access to mono and dually labelled rna probes for enzymatic assays and in vivo translation. *Nucleic Acids Research*, 50(1):e3–e3, 2022.
13. Note1. Here each point corresponds to 200 frames acquired over a minute.
14. Yu Ohsugi and Masataka Kinjo. Multipoint fluorescence correlation spectroscopy with total internal reflection fluorescence microscope. *Journal of Biomedical Optics*, 14(1):014030–014030, 2009.

-
15. readPTUFLIM.
https://github.com/TKmist/readPTU_FLIM/tree/NIKON_correction.
 16. Vladana Vukojević, Marcus Heidkamp, Yu Ming, Björn Johansson, Lars Terenius, and Rudolf Rigler. Quantitative single-molecule imaging by confocal laser scanning microscopy. *Proceedings of the National Academy of Sciences*, 105(47):18176–18181, 2008.
 17. Michael Wahl and Sandra Orthaus-Müller. Time tagged time-resolved fluorescence data collection in life sciences. *Technical Note. PicoQuant GmbH, Germany*, 2:1–10, 2014.
 18. Johtaro Yamamoto, Shintaro Mikuni, and Masataka Kinjo. Multipoint fluorescence correlation spectroscopy using spatial light modulator. *Biomedical Optics Express*, 9(12):5881–5890, 2018.

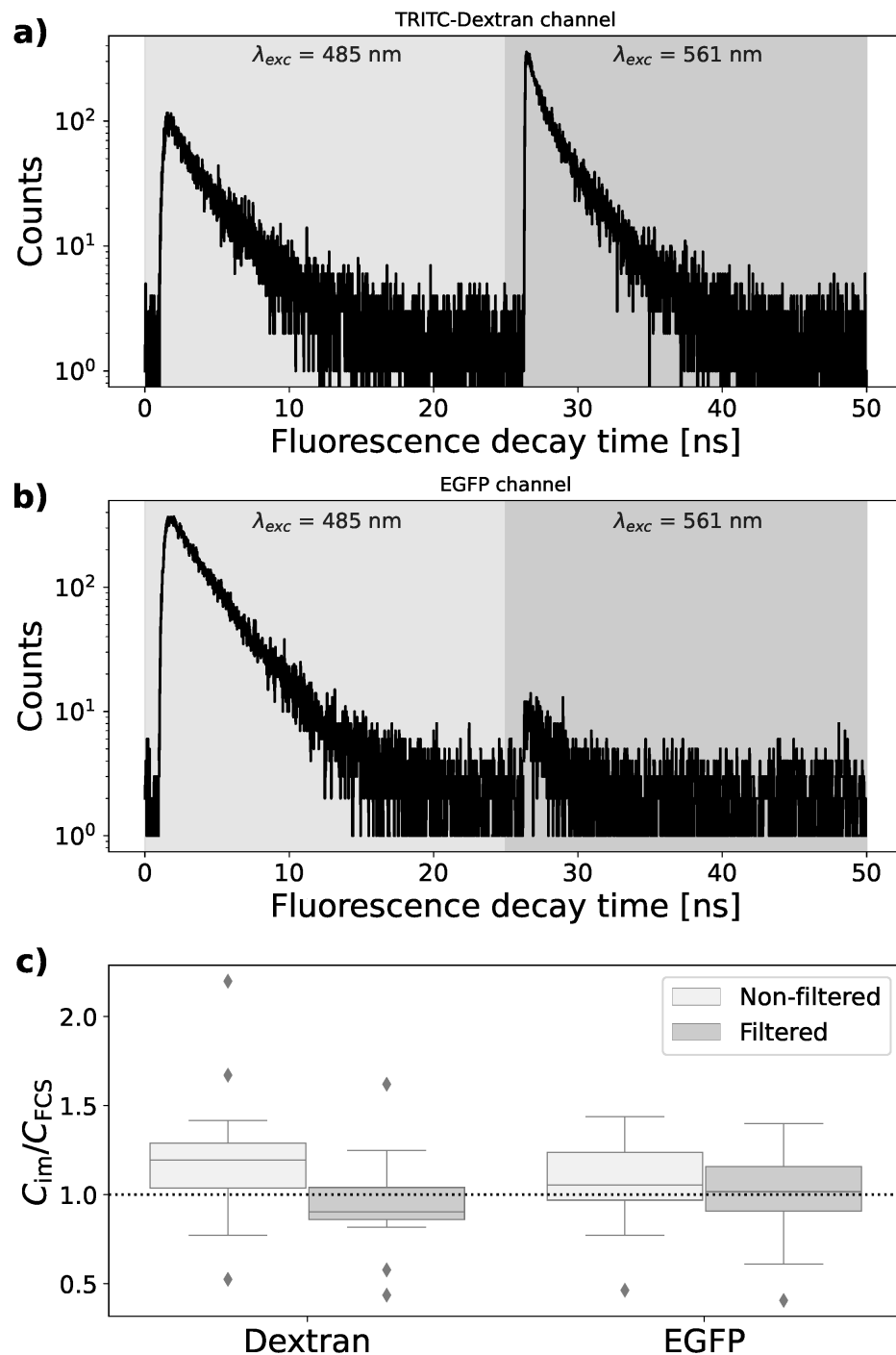


Figure 4. Figure a depicts raw fluorescence decay patterns acquired in the pulse interleaved excitation, PIE, mode in living cells where two fluorophores (EGFP and TRITC-labeled dextran) were present. Although the photons were registered in the TRITC channel, some GFP molecules were excited due to the long tail of the excitation spectra of the fluorescent protein. By analogy, Figure b depicts fluorescence decay for the photons registered in the EGFP channel. Here, part of the TRITC molecules were also excited by the 485 laser. Figure c shows boxplots comparing the filtered and non-filtered data of the fluorescence signal. The filtering was done using a simple time-gating method, which involves selecting the photons that fall into the selected decay-time range.

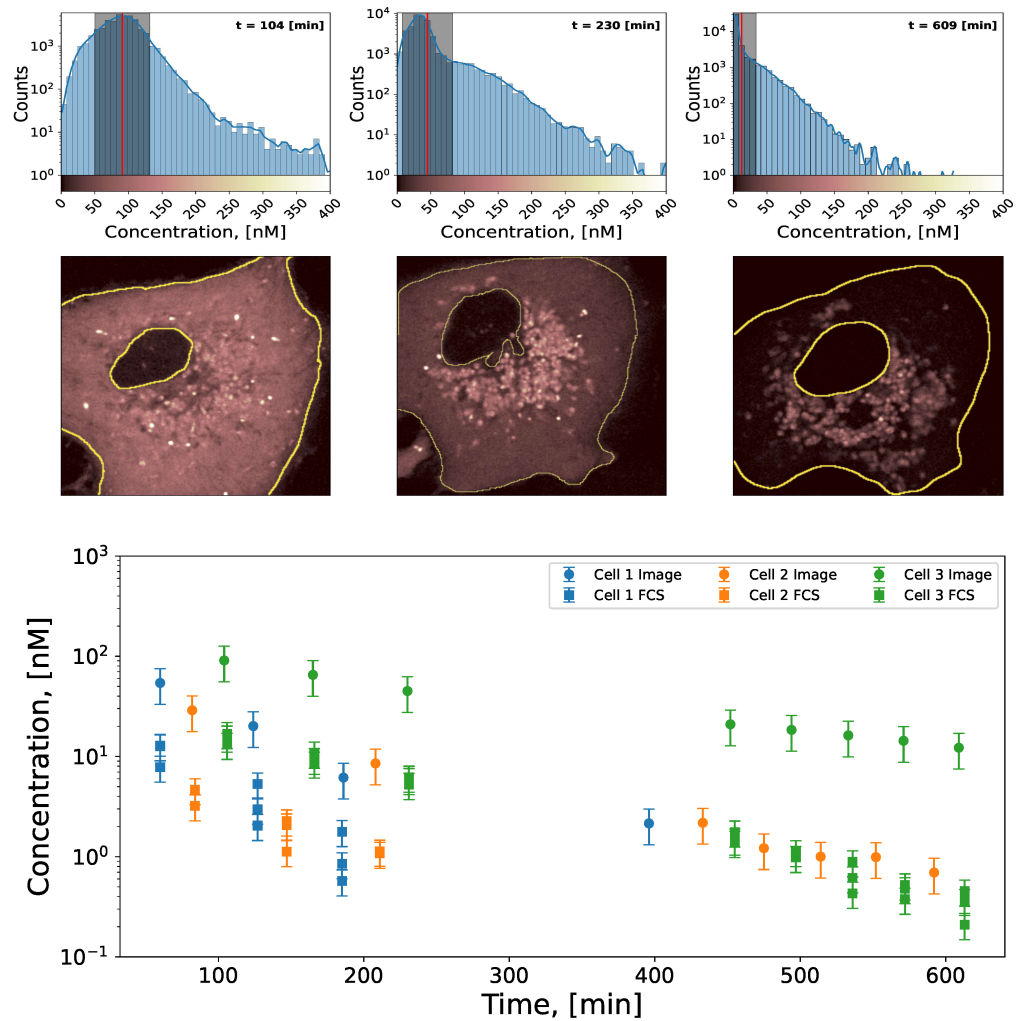


Figure 5. The top panel of the figure shows histograms of the concentration calculated for each image pixel. The calculations were restricted to the ROI marked with yellow lines on the images below the histograms. The histograms and images represent the data for a single cell tracked in time (cell 3) at $t = 104$, 230, and 609 minutes after the mRNA injection into the cells. The red line represents the mean concentration value, and the shading corresponds to the square root of the data variance. The plot below the images depicts the tracking of the changes in mRNA concentration in time for three cells.

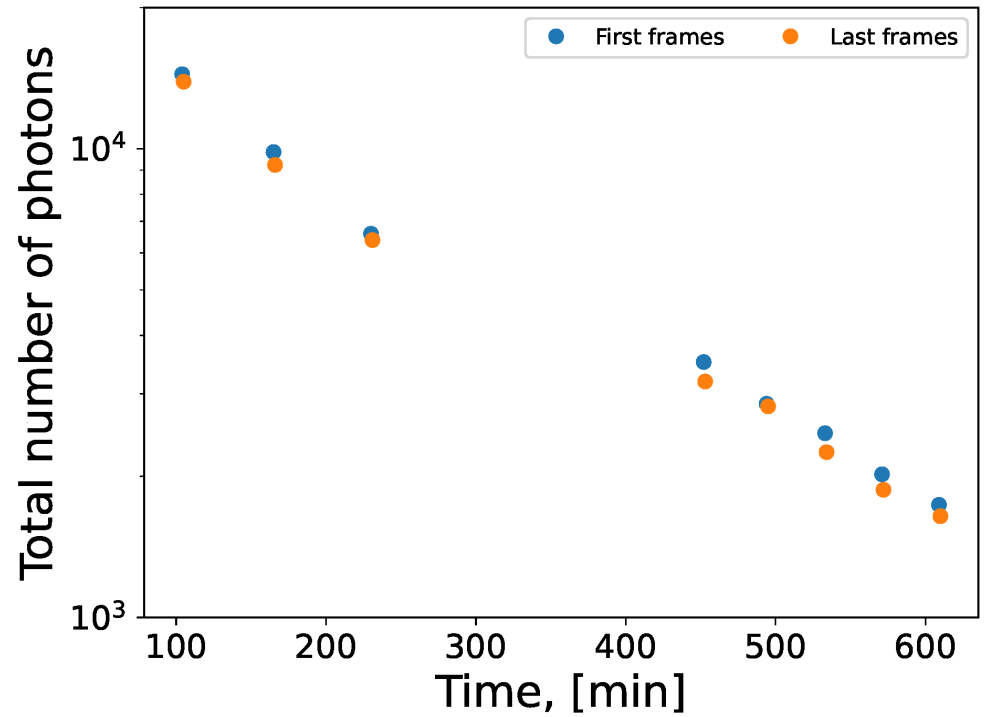


Figure 6. Figure shows the time changes in the total number of photons registered in the region of interest for a single cell (cell 3). We compared the total number of photons registered during the first and the last frame of each time data point. During the acquisition of the frames, a small drop in the total number of photons was observed, probably due to the photobleaching of the dyes, even though we reduced the laser power and the dwell time. The drop between the first and last frames was, however, too small to be considered the main source of the decay in the number of photons observed over the entire experiment (more than ten hours).

